

## Energy Loss and Drag in a Steady Flow through Emergent Vegetation

*Ghufran Ahmed Pasha<sup>1</sup>, Prof. Norio Tanaka<sup>1,2</sup>*

1. Graduate School of Science and Engineering, Saitama University

2. International Institute for Resilient Society, Saitama University  
Saitama, Japan

### ABSTRACT

Floods resulting from extreme events like tsunami may inundate widespread inland area. Although rigid shielding infrastructure (hard protection structures) such as flood protection walls reduce flood risks, but these structures may fail if flow conditions exceed the design threshold. Vegetation (forest) can act as a natural buffer zone to reduce the inundation area and dissipate energy of flowing water. The present paper summarizes a series of laboratory experiments where the energy loss through emergent vegetation was investigated. The energy loss was determined against vegetation of constant thickness, changing density and initial Froude number. The results highlight the significant effect of denser vegetation on energy loss.

**KEY WORDS:** Tsunami; Vegetation; Forest density; Steady Flow; Backwater rise; Energy Loss; Drag coefficient

### INTRODUCTION

Various researchers have worked in the recent years to derive the best possible method for tsunami mitigation. Artificial methods (hard solutions) like construction of sea walls & embankments, installing tsunami gates, putting up breakwater structures etc can prove to be costly for developing countries as it requires huge capital investment (Tanaka, 2009). Further, tsunami has a possibility to exceed the designed capacity of artificial structure.

Coastal forests have proved to be a vital solution in mitigating catastrophic coastal phenomena like tsunami and storm surges. Previous studies have also shown by post-tsunami surveys that coastal trees helped to reduce the damaging effects of natural disasters (Kathiresan and Rajendran, 2005; Tanaka et al., 2007; Mascarenhas and Jayakumar, 2008). A forest can offer sufficient resistance to a tsunami force depending upon its structure and density. Iimura and Tanaka (2012) investigated the effect of vegetation density both experimentally and analytically and confirmed that both the level and velocity of the water behind the vegetation are reduced considerably by increasing the density of vegetation.

However, no research has been done in order to quantify the amount of energy loss due to vegetation itself. Vegetation thickness and forest densities are one of the vital parameters to be investigated. The energy reduction behind vegetation is discussed by many researchers (Thuy et al., 2009; Iimura and Tanaka, 2012) but energy reduction due to hydraulic jump formed behind vegetation has never

been studied previously. In this study, laboratory experiments were conducted in a flume to figure out the amount of energy loss through emergent vegetation of constant thickness, changing density and initial Froude number. This study will help in deciding forest width in relation to different flow conditions and vegetation arrangements.

### EXPERIMENTAL SETUP AND CONDITIONS

#### Experimental Procedure and Flume Characteristics

Laboratory experiments for 3 different cases (Table 1) were conducted in a water flume (constant bed slope 1/500), which is 5m in length, 0.7m in width, and 0.5m in height, in Saitama University. In an experimental channel, the ground conditions and tsunami characteristics implicated were not specific to any location but were considered in general. Froude similarity was applied to set the flow condition for the model scale (1/100) of the physical experiment. In the current study, as a first step, the initial Froude number ( $F_o$ , where reference velocity and water depth are used without a vegetation model placed in a channel) was set around 0.55-0.75 representing steady flow conditions. The water depths selected in the experiment were 3, 3.5, 4, 4.5, 5, 5.5, 6, 6.5, 7, 7.5 cm at the channel start, setting the  $F_o$  approximately equal to 0.55-0.75.

After mounting the full width of forest model about 2.5m from the upstream inlet, the water level was measured throughout the center of the channel by using a point gauge. Using flow meter (Signet 8150 Flow Totalizer), the discharge value ( $Q$ ) was measured. Mean velocity was computed using the measured water depth and discharge. The water velocity calculated from flow meter discharge reading was compared with the depth averaged velocity calculated from particle image velocimetry (PIV) (Laser Light Sheet: G200, high speed digital CCD camera: K-II, fps: 600, flow analyzing software: FlowExpert2D2C, Katokoken Co., Ltd.). The difference was less than 5%. The drag force on individual cylinder was measured using a two-axis load cell (SSK Co., model LB60) having resolution of 1/1000 and can measure 1N for the maximum load. In addition to measure the drag force, a gap is required between individual cylinder and the channel bottom. The experiments were conducted with the smallest possible gap, 0.001m, similar to the measurement by Takemura and Tanaka (2007).

#### Forest Conditions

The tree species selected for the forest model was the Japanese pine

tree (average tree height = 15m and trunk diameter = 0.4m) found on the Sendai Plain; the tree crown of which was high compared with the tsunami height, and can be considered as circular cylinders (Tanaka et al., 2014). For a 1/100 scale model, the trees were modeled by wooden cylinders with a diameter of 0.004m set in a staggered arrangement, based on the average diameter of pine trees. Fig. 1 and Table 1 show the details of vegetation arrangement where  $D$  is the distance between cylinders and  $W$  is the width of vegetation model. According to Takemura and Tanaka (2007), flow structures are different depending upon the  $G/d$  arrangement of forest model (forest density), where  $G$  represents the spacing between each cylinder in a cross-stream direction, and  $d$  is the diameter of a cylinder (Fig. 1). The  $G/d$  ratio also indicates whether a forest is sparse or dense. In order to investigate the energy loss through vegetation, forests with 3 different values of  $G/d$  (0.25, 1.09 and 2.13) were made.  $D$  and  $W$  were determined under same vegetation thickness:  $dn$  which is defined by a product of the diameter of breast height of tree and no. of trees in a rectangle with a frontage of unit length along shoreline and depth equal to width of forest ( $W$ ) (Fig. 1), (Shuto, 1987). In this study  $dn$  was calculated as:

$$dn = \frac{2}{\sqrt{3}D^2} Wd \times 10^4 \quad (1)$$

Where  $10^4$  in above equation adjust a unit in Shuto's definition of  $dn$  because  $D$  and  $W$  are in cm, and  $d$  (0.004) is in m. In the experiment  $dn$  was set ~380 in all experiments. As the forest density increases, the width of vegetation becomes narrower because  $dn$  is fixed.

Table 1 Experimental Conditions

Case No.	$F_o$	$G/d$	$D$ (cm)	$W$ (cm)	$dn$ (No. cm)	Forest Type
1	0.57, 0.62, 0.65, 0.66, 0.68, 0.69, 0.70, 0.71, 0.73	0.25	1	8.23	380	Dense
2	0.57, 0.62, 0.65, 0.66, 0.68, 0.69, 0.70, 0.71, 0.73	1.09	1.67	23.60	391	Intermediate
3	0.57, 0.62, 0.65, 0.66, 0.68, 0.69, 0.70, 0.71, 0.73	2.13	2.5	52.48	388	Sparse

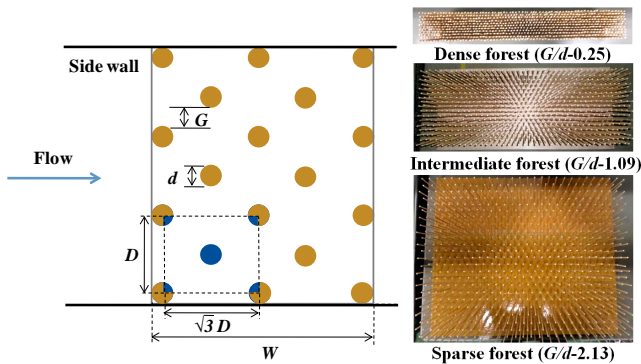


Fig. 1 Detailed arrangement and the definition of forest model

## Non-dimensional pi groups

Using Buckingham's Pi theorem, the following dimensionless groups were developed:

$$f \left[ \frac{b}{h_o}, \frac{\Delta h}{h_o}, \frac{V_o}{\sqrt{gh_o}}, \frac{V_1}{\sqrt{gh_1}}, \frac{\rho_w h_o V_o}{\mu}, \frac{G}{d}, dn, \frac{y_2}{y_1}, \frac{LJ}{y_1}, \frac{V_2}{V_1}, \frac{\Delta E_1}{E_1}, \frac{\Delta E_2}{y_1} \right] = 0 \quad (2)$$

Where,  $b$  = channel width,  $h_o$  = initial water depth without forest,  $\Delta h$  = backwater rise,  $V_o$  = velocity at  $h_o$ ,  $F_o$  = Froude number at  $h_o$ ,  $F_{US}$  = Froude number on the upstream of forest against water depth  $h_1$  and velocity  $V_1$ ,  $g$  = gravitational acceleration,  $\rho_w$  = density of water,  $\mu$  = viscosity of water,  $y_1$  = minimum water depth during the jump,  $y_2$  = mean water depth after the hydraulic jump,  $LJ$  = length of hydraulic jump,  $V_2$  = mean velocity after hydraulic jump,  $HGL$  = hydraulic grade line,  $EGL$  = energy grade line,  $E_1$  = specific energy at forest front,  $E_2$  = mean specific energy after formation of hydraulic jump where the flow is sub-critical,  $\Delta E_1$  = total energy loss ( $E_1 - E_2$ ) and  $\Delta E_2$  = energy loss due to hydraulic jump  $[(y_2 - y_1)^3 / 4y_1 y_2]$  (Figs. 1~2).

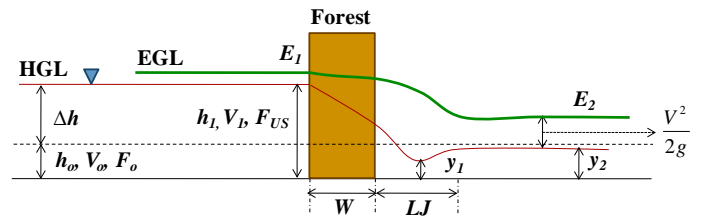


Fig. 2 Flow structure scheme and definition of various parameters

Since width of channel ( $b$ ) is same for every case during the experiment, so first pi group can be ignored. In addition, viscosity and density of water are same for every case and Froude scaling is commonly used for free surface gravity flows, thus pi-5 group which is Reynold's number, is also ignored. Therefore, energy loss is mainly a function of initial Froude's number ( $F_o$ ) and forest density ( $G/d$ );

$$\frac{\Delta E_1}{E_1}, \frac{\Delta E_2}{y_1} = f \left[ \frac{V_o}{\sqrt{gh_o}}, \frac{G}{d} \right] \quad (3)$$

## RESULTS AND DISCUSSIONS

### Effect of forest density and Froude number on backwater rise

Increasing the density of a forest raises the maximum water level in front of the forest, and increases the water surface slope inside the forest (Iimura and Tanaka, 2012). It can be seen from Fig. 3 that backwater rise is lower for the sparse forest conditions ( $G/d = 2.13$ ) as compared to dense conditions ( $G/d = 0.25$ ) for a given Froude number. Dense arrangement of trees exhibit a higher flow resistance compared to sparse arrangement and consequently results in a higher back water rise.

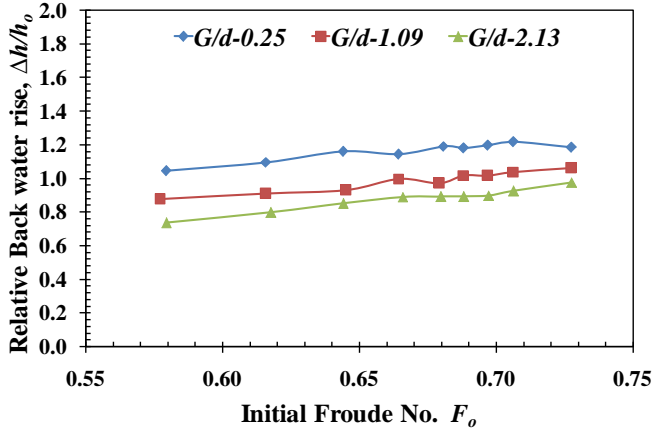


Fig. 3: Relative Backwater rise  $\Delta h/h_o$  for three different forest densities ( $G/d$ ) and initial Froude numbers ( $F_o$ )

The initial flow conditions without forest model placement in the channel was varied between  $F_o = 0.55$  and  $F_o = 0.75$ . After placing the forest in the channel, the water level at forest front increased and the water surface slope inside the vegetation became larger (Fig. 4). Relative backwater rise which is the ratio of backwater rise to initial flow depth, slightly increased with increasing initial Froude conditions. This shows that initial flow depth has very little effect on the relative backwater rise for a given Froude number.

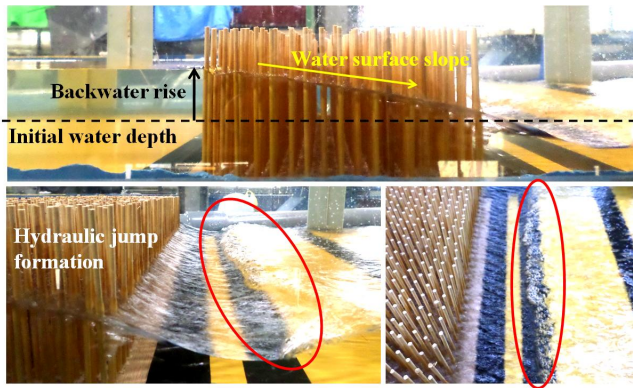


Fig. 4 Flow phenomenon

### Energy reduction behind vegetation

Hydraulic resistance and reflection of water from trees can reduce energy of flowing water, inundation depth, inundation area and hydraulic force behind the forest. The water passing through the forest becomes weaker which results in minimizing damage behind the forest. However, understanding hydraulic resistance of forest needs to be further investigated.

As the tree density increases (i.e., vegetation width becomes smaller), the maximum water level and maximum velocity behind the vegetation decrease (Imura and Tanaka, 2012). In the current study, the water level was measured at the channel center and throughout the length of channel. The specific energy which is defined as the energy per pound of water at any section of a channel measured with respect to channel bottom (Chow, 1959).

$$E = y + \alpha \frac{V^2}{2g} \quad (4)$$

Where;  $E$  is specific energy,  $y$  is water depth,  $V$  is velocity and  $\alpha$  is coefficient to account for variation in velocity. In the current study the value of  $\alpha$  is considered as 1. Since the flow is steady, therefore against the known discharge ( $Q$ ), mean velocity was calculated using relationship  $V=Q/A$ . A clear difference of water depths on upstream ( $U/S$ ) and downstream ( $D/S$ ) of vegetation was observed which resulted in an energy loss to a certain extent (Fig. 4). The energy loss ( $\Delta E$ ) through vegetation is the difference between specific energy upstream and downstream of vegetation.

With increasing the forest density, the water level was increased in front of vegetation by reflection and damming up (Imura and Tanaka, 2012, Pasha and Tanaka, 2016). Under the current conditions, the water flow passing through the vegetation became critical just  $D/S$  of vegetation, which resulted in a formation of undular hydraulic jump. Although the intensity of hydraulic jump was small, still it contributed to energy loss to some extent. In the present study, the energy loss is subdivided into two portions:

1. Total energy loss ( $\Delta E_1 = E_1 - E_2$ )
2. Energy loss due to hydraulic jump ( $\Delta E_2 = (y_2 - y_1)^3 / 4y_1y_2$ )

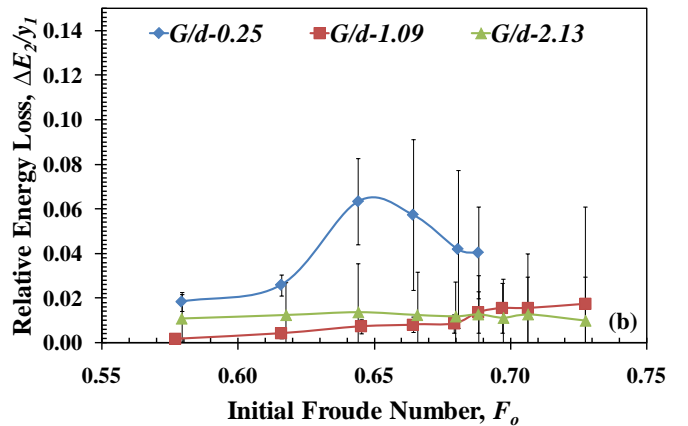
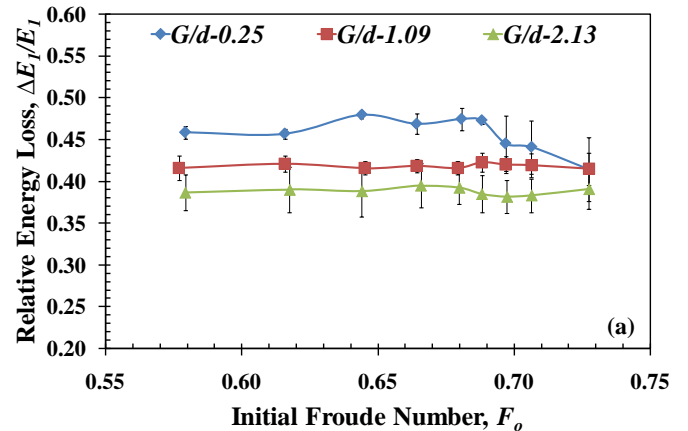


Fig. 5 Relative energy loss for three different forest densities ( $G/d$ ) and initial Froude numbers ( $F_o$ ) (a) Total energy loss, (b) Energy loss due to hydraulic jump

Where  $E_1$  is specific energy at forest front,  $E_2$  is mean specific energy after formation of hydraulic jump where the flow is sub-critical,  $y_1$  = minimum water depth during the jump,  $y_2$  = mean water depth after the hydraulic jump. The mean values of  $E_2$  and  $y_2$  are considered because of the fluctuations in water surface after the hydraulic jump.

Fig. 5a shows the relationship between the relative total energy loss ( $\Delta E_1/E_1$ ) and the initial Froude number. This figure shows the total energy reduction due to forest and due to hydraulic jump. It is clear from the Fig. 5a that total relative energy loss is greater for dense forest and least for the sparse forest. However relative total energy loss almost remained constant when initial Froude number was increased from 0.55 to 0.75. Vertical bars represent standard deviation.

In case of dense arrangement ( $G/d=0.25$ ), the last three plotted points showed comparatively low value of energy reduction (Fig. 5a). This is because the length of hydraulic jump increased with increasing the Froude number and for these three plots, the length of jump exceeded the available channel length downstream of forest model. In such a case  $E_2$  was calculated against super critical flow conditions which resulted in low energy reduction. This shows the contribution of hydraulic jump in energy reduction.

Fig. 5b shows the relationship between the relative energy loss due to hydraulic jump ( $\Delta E_2/y_1$ ) with the initial Froude number. For most of the experimental conditions, breaking undular hydraulic jump was formed in case of dense vegetation while non breaking undular jump occurred against the intermediate and sparse vegetation. The intensity of hydraulic jump was also increased by increasing the Froude number. The maximum energy reduction due to undular jump reached 6.34% for dense conditions which reduced to 1.74% and 1.38% for intermediate and sparse conditions, respectively. Fig. 5b also shows that, at low Froude number flow, the difference in energy reduction by sparse forest was slightly higher compared to intermediate forest because mean water depth  $y_2$  was greater for sparse forest compared to intermediate forest. Against same vegetation thickness, higher forest density (lesser width) resulted in higher energy loss; therefore considerable width of land can be saved by adopting dense forest arrangements.

### Variation of drag coefficient with forest density and Froude number:

The drag coefficient  $C_d$  for each solid circular cylinder is defined as:

$$C_d = \frac{2F}{\rho U^2 dH} \quad (5)$$

Here,  $F$  (N) is drag force on individual centrally positioned cylinder at forest front,  $\rho$  ( $\text{kg/m}^3$ ) is the fluid density,  $d$  (m) is diameter of cylinder and  $H$  (m) is water depth in front of cylinder.  $U$  (m/s) is the calculated mean velocity against water depth  $H$  (m) and discharge  $Q$  ( $\text{m}^3/\text{s}$ ). The relationship between drag coefficient of cylinder and initial Froude number against different forest densities is shown in Fig. 6. Against all the sub-critical flow conditions (Froude No. 0.55 - 0.75), the drag coefficient increased slightly by increasing the Froude number. However, for the last three values of  $F_o$  ( $G/d = 0.25$ ) the drag coefficient abruptly increased due to occurrence of cylinder oscillations. During oscillations, additional mass acts on the cylinder which resulted in higher drag force. Among the three forest densities, dense forest showed maximum drag coefficient which started to reduce as the spacing between the cylinders was increased (sparse forest).

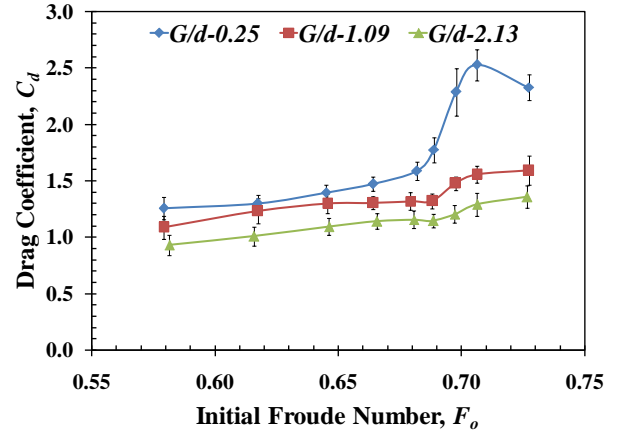


Fig. 6 Drag Coefficient of individual cylinder at forest front for three different forest densities ( $G/d$ ) and initial Froude numbers ( $F_o$ )

### CONCLUSIONS

Against constant vegetation thickness  $dn$ , on the upstream of vegetation model, the backwater rise was found to increase by increasing the density of forest due to higher vegetation resistance. Contrarily on the downstream side, energy was lost due to forest resistance and due to formation of undular hydraulic jump. The maximum energy loss in case of dense vegetation arrangement ( $G/d=0.25$ ) reached 6.34% by breaking undular hydraulic jump. However, with increase in spacing between cylinders ( $G/d=2.15$ ), the maximum amount of energy loss reduced to 1.38% due to non-breaking undular hydraulic jump. The drag coefficient ( $C_d$ ) of vegetation was also reduced by decreasing the forest density.

The findings are important for optimum forest design, as dense arrangement can save considerable width of land in order to reduce the maximum energy. In the future, more experimental study is required for high Froude number flow in order to further investigate the phenomena.

### ACKNOWLEDGEMENTS

This study was funded by a JSPS Grant-in-Aid for Scientific Research (No. 15H02987).

### REFERENCES

Chow, V.T. (1959). Open Channel Hydraulics. McGraw-Hill, New York, NY: 41.  
 Iimura, K. and Tanaka, N. (2012). Numerical simulation estimating the effects of tree density distribution in coastal forest on tsunami mitigation. *Ocean Engineering* 54: 223-232.  
 Pasha, G.A., Tanaka, N. (2016). Effectiveness of finite length inland forest in trapping tsunami-borne wood debris. *Journal of Earthquake and Tsunami* 10 (2), 1650008: 1-26.  
 Kathiresan, K. and Rajendran, N. (2005). Coastal mangrove forests mitigated tsunami. *Estuar. Coast. Shelf Sci.* 65 (3): 601-606.  
 Mascarenhas, A. and Jayakumar, S. (2008). An environmental perspective of the post-tsunami scenario along the coast of Tamil Nadu, India: role of sand dunes and forests. *J. Env. Manage.* 89: 24-34.

Shuto, N. (1987). The effectiveness and limit of tsunami control forests. *Coastal Eng. Japan* 30 (1): 143-153.

Takemura, T. and Tanaka, N. (2007). Flow structures and drag characteristics of a colony-type emergent roughness model mounted on a flat plate in uniform flow. *Fluid Dynamics Research* 39: 694-710.

Tanaka, N. (2009). Vegetation bioshields for tsunami mitigation: Review of the effectiveness, limitations, construction, and sustainable management. *Lands. Ecol. Eng.* 5: 71-79.

Tanaka, N., Sasaki, Y., Mowjood, M.I.M., Jinadasa, K.B.S.N. and Homchuen, S. (2007). Coastal vegetation structures and their

functions in tsunami protection: experience of the recent Indian Ocean tsunami. *Lands. Ecol. Eng.* 3: 33-45.

Tanaka, N., Yasuda, S., Iimura, K. and Yagisawa, J. (2014). Combined effects of coastal forest and sea embankment on reducing the washout region of houses in the Great East Japan tsunami. *Journal of Hydro-environment Research* 8: 270-280.

Thuy, N.B., Tanimoto, K., Tanaka, N., Harada, K. and Iimura, K. (2009). Effect of open gap in coastal forest on tsunami run-up - investigations by experiment and numerical simulation. *Ocean Engineering* 36: 1258-1269.

### Appendix

